


 Cite this: *RSC Adv.*, 2021, **11**, 31590

## Microwave-driven hydrogen production (MDHP) from water and activated carbons (ACs). Application to wastewaters and seawater

 Satoshi Horikoshi, <sup>a</sup> Leo Takahashi, <sup>a</sup> Kirara Sueishi, <sup>a</sup> Honoka Tanizawa <sup>a</sup> and Nick Serpone <sup>b</sup>

This article reports on low-temperature steam reforming and water–gas shift processes to generate hydrogen efficiently when water is passed through microwave-heated activated carbon (AC) particulates, in contrast to conventional steam reforming that is not particularly efficient at temperatures around 600 °C. The microwave-driven method performed efficiently at this temperature producing hydrogen with yields of 70% or more, as a result of the microscopic local microwave heating of the AC particulates. To the extent that the activated carbon is produced from plant biomass-related raw materials, the carbon dioxide produced is carbon neutral. Conditions for hydrogen generation were optimized with regard to the size of the AC particles, the water flow rate, and the size of the reactor. For practical applications of this microwave-based method, hydrogen was also generated efficiently with yields of 75–80% when using spent activated carbons (large size distribution) and model contaminated wastewaters and artificial seawater; significant energy was saved under the conditions used. The re-use of spent ACs eliminates the need for their disposal after being used in water and sewage treatments. In addition, the presence of any organic matter in wastewaters is also a likely effective source of hydrogen (yields, 75–85%). And not least, although generation of hydrogen from seawater is a difficult electrolytic process, the microwave method proved to be an attractive and efficient technology toward hydrogen generation from seawater with yields of 85 to 90%. Addition of Pt deposits on the activated carbon support, however, provided no advantages over pristine AC particulates.

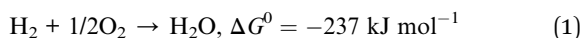
 Received 7th August 2021  
 Accepted 9th September 2021

DOI: 10.1039/d1ra05977g

[rsc.li/rsc-advances](http://rsc.li/rsc-advances)

## 1 Introduction

Reaction of 2 mols of hydrogen with 1/2 mol of oxygen yields 1 mol of water exothermally with a standard Gibbs free energy of 237 kJ mol<sup>-1</sup> at 298 K (eqn (1)).



From this point of view, hydrogen has attracted considerable attention as a clean energy source. Additionally, the energy density per weight of hydrogen gas is high (142 MJ kg<sup>-1</sup>) compared with other fuels (*e.g.*, gasoline, 49 MJ kg<sup>-1</sup>), whereas the energy density per volume is rather low (11.9 MJ m<sup>-3</sup> *versus* 34.6 MJ m<sup>-3</sup> for gasoline).<sup>1</sup> Relative to liquefied natural gas (39.0 MJ m<sup>-3</sup>), the volume energy density of hydrogen is about a quarter, whereas when compared on a weight basis (55 MJ kg<sup>-1</sup>) it is about threefold greater. The hydrogen is also a raw

material for very basic chemical substances such as in the synthesis of ammonia and methanol; it is also used in large quantities for petroleum refining. However, the bulk of hydrogen used is mainly produced from fossil resources such as petroleum, coal and natural gas, all of which are energy fuel sources in their own right. Hydrogen energy obtained from such fossil fuels is not desirable as a means of realizing a clean and sustainable energy source. Accordingly, a new way of thinking that would yield a practical hydrogen extraction method is significantly desirable that would implicate a wider hydrogen resource, namely the decomposition of water.

In this regard, Nicholson and Carlisle were the first to report the electrolysis of water (*ca.* 1800) using a voltaic pile following the discovery of electricity by Alessandro Volta.<sup>2</sup> Although making hydrogen and oxygen from electrolysis of water is now considered a very simple method, the problem is that it takes an energy source (electricity) to break down water into another energy vector: hydrogen, which when used in a fuel cell converts the hydrogen energy back into electrical energy. Accordingly, the balance between electrical energy consumed and electrical energy produced is an important consideration. The early days (1986–1998) witnessed electricity being generated in Niagara, Canada, to electrolyze water to extract hydrogen, which was

<sup>a</sup>Department of Materials and Life Sciences, Faculty of Science and Technology, Sophia University, 7-1 Kioicho, Chiyodaku, Tokyo 102-8554, Japan. E-mail: horikosi@sophia.ac.jp

<sup>b</sup>PhotoGreen Laboratory, Dipartimento di Chimica, Università di Pavia, Via Taramelli 12, Pavia 27100, Italy. E-mail: nick.serpone@unipv.it



then liquefied by the organic hydride route and subsequently transported to Germany.<sup>3</sup>

Some four decades ago, Fujishima and Honda demonstrated that hydrogen could be produced photoelectrochemically by the water-splitting process using  $\text{TiO}_2$  as the photocatalytic electrode, a method that would minimize the use of electrical energy.<sup>4</sup> Hydrogen can also be produced by the direct thermal decomposition of water, although this process would require temperatures greater than 4000 °C, available only from nuclear reactors.<sup>5</sup> In contrast, the photocatalytic decomposition of water using the  $\text{TiO}_2$  photocatalyst would require only light energy equal to or greater than the bandgap (3.2 eV; anatase  $\text{TiO}_2$ ; *i.e.*, less than 387 nm) so that water could, in principle, be decomposed even by means of sunlight UVA radiation. It is significant that hydrogen can be extracted from an available inexpensive natural source (water) and sunlight, even though this photo-assisted process is currently impractical in a large scale because the energy conversion efficiency is rather low (0.4%) owing to several factors.<sup>6</sup> Nonetheless, research on the possibility of hydrogen generation from the photodecomposition of water continues unabated.<sup>7</sup>

Attempts have been made to reduce the consumption of energy by selective heating of solid catalysts with microwaves in the last two decades.<sup>8</sup> Most recently, Jie and coworkers<sup>9</sup> reported on the production of hydrogen from plastics (plastic bags, bottles and packaging) by selective microwave-heating of the catalysts. A concept of converting plastics and trap grease (a waste material recovered from traps on sewer lines) pyrolytically at *ca.* 850 °C *via* a two-stage process was proposed nearly two decades ago by Czernik and coworkers<sup>10</sup>: (i) fast pyrolysis to convert polymers to a gas/vapor stream of monomers and other low-molecular weight compounds followed by (ii) catalytic steam reforming of this gas to yield hydrogen and carbon oxides. In fact, the first commercial plant of turning plastics into hydrogen built in northwest England is close to operation.<sup>11</sup> Typically, the process involves pulverizing the plastics, followed by mixing with a catalyst made of iron oxide and aluminum oxide, and subsequently irradiated with 1000 W microwaves. The microwaves trigger the catalyst particles to strip over 97% of the hydrogen from the plastic in seconds. The process uses less energy because it only heats the catalyst, not all the plastics; most of the black residue left behind consists of carbon nanotubes, a valuable material for electronics and other uses.

Along similar lines, our previous research pointed out that the use of microwaves can save energy for the extraction of hydrogen from hydrogen-storage liquids,<sup>12</sup> to the extent that hydrogen is a gas and so it is inconvenient to store and transport. Accordingly, hydrogen gas is best stored when it is chemically bonded to such organics as toluene *via* a hydrogenation reaction, and transported in the form of methylcyclohexane. Whenever hydrogen gas is needed, it can be extracted by a dehydrogenation reaction in the presence of a Pt catalyst.<sup>12</sup> However, as the dehydrogenation reaction is an endothermic process, it is necessary to heat the Pt catalyst to obtain hydrogen that could be achieved using the exhaust heat from an incinerator. A more elegant method was suggested earlier by us<sup>12</sup> in which the heat could be supplied by

microwaves that implicated the selective heating of the Pt catalyst supported on activated carbon particles using microwaves, referred to as the microwave-driven organic hydride (MDOH) method. Inasmuch as the hydrogen-storage liquids methylcyclohexane and toluene are non-polar solvents, they do not absorb the microwaves so that microwaves are used only for heating the catalyst selectively, an energy-saving effect. Comparing conventional heating and microwave heating, the power consumption required for catalyst heating can be reduced to 1/17 with the microwaves. In this way, the hydrogen acquisition technology may be improved significantly over the traditional heating methods.

The results reported herein were discovered rather serendipitously when we inadvertently introduced ion-exchanged water instead of methylcyclohexane into a microwave-heated Pt/AC catalyst system during a MDOH experiment. Normally that would have not occurred had we not been required to wear facial masks owing to the Covid-19 virus, as the smell of this organic substrate is rather obvious from odorless water. It was only after about 20 min that we noticed the inadvertent misstep, yet the gas chromatograph detected hydrogen continuously through this time that could only be attributed to a process involving the flowing water. This led us to investigate the process further with regard to (i) the elucidation of the principle of hydrogen generation from water *via* microwave irradiation, (ii) the search for the optimal conditions to generate hydrogen, (iii) the examination of hydrogen generation efficiency in the presence of catalysts and (iv) the extent to which the microwaves were absorbed. In addition, the extent of hydrogen production from contaminated waters and seawater was also examined with the perspective of using waste activated carbon from water and sewage treatment plants.

## 2 Experimental methods

### 2.1 Microwave device setup

The system used toward the microwave-driven hydrogen production (MDHP) from wastewaters and seawater is displayed in Fig. 1a and b; it included a short plunger, an electric field monitor, power sensors, an *E/H* tuner (*E*, electric field; *H*, magnetic field) and an air-cooling isolator. The incident and reflected waves of the microwave radiation were measured precisely with a power meter (E4419B EPM series dual-channel power meter, Keysight Technologies, Santa Rosa, CA, USA) and a power sensor (E9300A E-series average power sensor, Keysight Technologies, Santa Rosa, CA, USA), respectively. The microwave irradiation setup further consisted of a single-mode cavity  $\text{TEM}_{103}$  (transverse electric mode 103) used to irradiate the reactor contents. Note that the single-mode applicator refers to the waveguide between the iris and the short plunger, and the  $\text{TE}_{103}$  indicates that 1.5 wavelength microwaves resonate between the iris and the short plunger.

Continuous microwave radiation was generated within a very narrow frequency (2.45000 GHz) from a microwave generator using a GaN semiconductor (GEAP-A003A01, LeanFa Srl, Ruvo di Puglia, Bari, Italy; maximum power, 250 W) that caused the microwaves to be suitably amplified by the resonator.<sup>13</sup> The



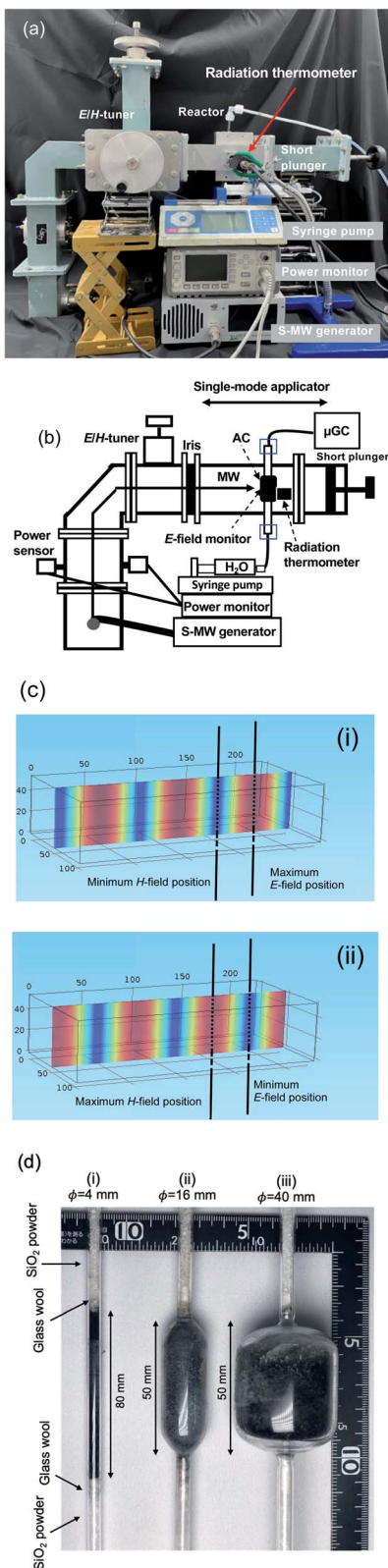


**Fig. 1** Photograph (a) and the schematic (b) of the microwave irradiation system consisting of a 2.45 GHz semiconductor microwave (S-MW) generator, an electric field (E-field) monitor, an E/H-tuner, and a short plunger, power monitors, an air-cooling isolator and a single-mode applicator; (c) distribution of the (i) E-field and the (ii) magnetic field H-field inside the single-mode applicator from the COMSOL Multiphysics 4.3a program with RF module; (d) picture of single-pass quartz fixed-bed tubular reactors containing activated carbon, SiO<sub>2</sub> powder, and glass wool.

wavelength of propagation of the microwaves in the TEM<sub>103</sub> mode within the waveguide was 14.78 cm (eqn (2)): <sup>14</sup>

$$\lambda = \frac{\lambda_0}{\sqrt{1 - (\lambda_0/2b)^2}} \quad (2)$$

where  $\lambda$  is the wavelength in the waveguide;  $\lambda_0$  (2.45 GHz) = 12.24 cm is the wavelength in vacuum given by  $c/f$ , { $c$  being the speed of light,  $2.9979 \times 10^{10}$  cm s<sup>-1</sup>, and  $f$  being the microwave frequency  $2.45 \times 10^9$  s<sup>-1</sup>, i.e. 2.45 GHz}; and  $b$  is the height of the waveguide (10.92 cm; Fig. 1b). The maximal position of the E-field from the iris was located at 3/4 the wavelength of the standing wave in the waveguide, namely at 11.09 cm.<sup>15</sup> However, the resonance differs depending on the reactor containing activated carbon and water together on the progress of the reaction. The resonance of the microwaves was adjusted with an E-field monitor, an E/H-tuner, and a short plunger at various wavelength cycles. The maximal position of the H-field from the iris was at half the wavelength of the standing wave in the waveguide, namely 7.39 cm.<sup>13</sup>

The distribution of the E- and H-field inside the single-mode applicator was calculated by using the COMSOL Multiphysics 4.3a program with the RF module (Fig. 1c). It is possible to predict whether the strength of the electric or magnetic field will be uniform above and below the applicator using a simulation technique. Therefore, the cylindrical quartz reactor installed at the position shown is uniformly irradiated with an electric or a magnetic field.

The three kinds of single-pass quartz fixed-bed tubular reactors with internal diameter of 4.0, 16 and 40 mm and 155 mm in length are shown in Fig. 1d. The activated carbon (AC particulates) was introduced into the vertical reactors; the upper and bottom parts of the reactors were then closed with glass wool and SiO<sub>2</sub> particles to prevent loss of the AC catalyst powder. The quantities of AC catalyst powder were such to fill the reactors at a height of *ca.* 80 mm for the 4 mm reactor (*ca.* 0.25 g) or *ca.* 50 mm for the 16 mm (*ca.* 4.5 g) and for the 40 mm (*ca.* 11.2 g) reactors. The activated carbon was from coconut shells manufactured by Fujifilm Wako Pure Chemical Industries, Ltd. To sort the sizes, the activated carbon was crushed using a mortar and six types of metal mesh sieves with dimensions <45 µm, 45–600 µm, 600–710 µm, 0.71–1.18 mm, 1.18–1.7 mm, and 1.7 mm. An elemental analysis (EDX-8100 ED) of the activated carbon revealed that it contained S (0.028%) and Zn (0.004%) in addition to C (99.968%).

The temperatures of the microwave-irradiated activated carbon were measured with a radiation thermometer (Japan sensor FLHX-TNE0220, temperature measurement range: 220–2000 °C; measurement time set at 0.001 s), with the focus of the radiation thermometer fixed at the center of the activated carbon phase. Note that since this radiation thermometer uses a wavelength of 0.8 to 2.6 µm, it can transmit 90% or more through the quartz glass and measure the temperature of the inclusions. The temperature of the activated carbon particulates at the inner reactor surface was measured by thermography (TVS-500, Nippon Avionics Co., Ltd.).

The ion-exchanged water (hydrogen carrier) was maintained at ambient temperature prior to being fed from the bottom part



of the single-pass continuous flow reactor using a syringe pump (Isis Co. Ltd., Fusion 100). The water was rapidly vaporized by the heated catalyst particulates subjected to microwave radiation. The dielectric loss of water is normally 8.03 at 30 °C, but decreases to 2.81 at 90 °C (ref. 16) and becomes zero for water vapor. Therefore, the temperature of the heated water is due to microwave heating and by the heat of the activated carbon.

For comparative purposes, experiments between microwave heating and conventional heating were also carried out under otherwise identical conditions of reactor, pump, and activated carbons in a ceramic electric tube furnace (Asahi Science Factory Co., ARF-16KC). The reactor was encased by the ceramic's heater, and to prevent loss of heat during the dehydrogenation process the whole setup was insulated from its surroundings with a glass fiber isolating jacket.

## 2.2 Analytical device and chemical reagents

Generated hydrogen gas was measured by gas chromatography (Agilent micro GC 490) using Ar as the carrier gas; the automatic analysis was continuously performed at 2 min intervals. The injector temperature was set to 100 °C; the injection time was set to 40 ms; the column temperature was set at 100 °C; the column pressure was set at 170 kPa. The maximal amount of hydrogen generated was theoretically calculated from the amount of water introduced by the syringe pump using a calibration curve; the latter was generated using 100% argon gas, a 1 : 1 hydrogen : argon mixed gas mixture, and 100% hydrogen gas (correlation coefficient  $R$  was 0.9994). Experiments for hydrogen gas generation were repeated twice; the difference between the two was less than 6%. The elemental analysis was performed by energy dispersive X-ray spectroscopy (EDX) using a Shimadzu Co. EDX-8100 ED spectrometer.

## 3 Results and discussion

### 3.1 Elucidation of the reaction events

The 4 mm quartz tube reactor was filled with *ca.* 0.25 g of the activated carbon (AC), following which the top and bottom were plugged with glass wool. The ion-exchanged water was introduced into the reactor at a flow rate of 0.1  $\text{mL min}^{-1}$  from the bottom of the reactor. The reactor was fixed at the maximal position of the electric field, such that the activated carbon could be heated almost exclusively by the microwave electric field (irradiation power, 15 W). Observations through the window on the side of the waveguide confirmed that the (black) activated carbon emitted red light as it was heated. Hydrogen was detected from the discharged gas by gas chromatography. A check of the reactor after 30 min indicated the amount of enclosed AC to have decreased (Fig. 2), suggesting that the introduced water reacted with the activated carbon to generate hydrogen. Passing the generated discharged gas through an aqueous solution of calcium hydroxide produced a white precipitate confirmed to be  $\text{CaCO}_3$  from the reaction:  $\text{Ca}(\text{OH})_2 + \text{CO}_2 \rightarrow \text{CaCO}_3 + \text{H}_2\text{O}$ , which is in line with the loss of activated carbon in the form of carbon dioxide. This result infers that hydrogen is generated after water encounters the microwave-

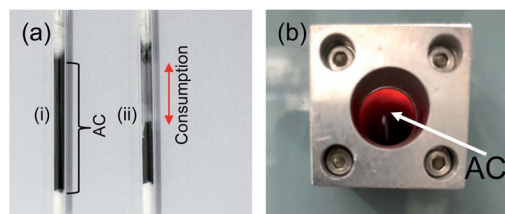
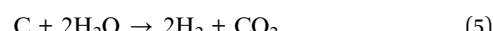


Fig. 2 (a) Photograph of the 4 mm reactor filled with activated carbon (AC): (i) before use, and (ii) after use (flow rate of  $\text{H}_2\text{O}$ : 0.1  $\text{mL min}^{-1}$ , microwave ( $E$ -field) input power: 15 W); (b) photograph of the AC in the single-mode applicator through the observation window for temperature measurement – note the red glow due to the microwave  $E$ -field heating.

hot activated carbon causing the gasification reaction to proceed yielding carbon monoxide and hydrogen (eqn (3)). No doubt, water was involved with carbon monoxide in a water–gas shift reaction (eqn (4)) to generate additional hydrogen together with carbon dioxide. Note that no carbon monoxide was detected by a gas chromatographic analysis at 600–700 °C, which infers that under the prevalent conditions CO was likely a short-lived transient intermediate in eqn (3) and (4):



or else (eqn (5)):



### 3.2 Optimal microwave conditions for $\text{H}_2$ generation

The optimal conditions for hydrogen generation involved a quartz tube filled with activated carbon (particulate size,  $<45 \mu\text{m}$ ; *ca.* 0.25 g) placed at the  $E$ -max and  $H$ -max positions for microwave irradiation in the single-mode applicator, subsequent to which the temperature of the activated carbon was monitored with respect to the microwave irradiation output (Fig. 3). Heating of the activated carbon proceeded quickly under  $E$ -field conditions, exceeding 460 °C by irradiation with 6 W microwaves rising to 750 °C when the microwave irradiation output was increased to 20 W. A further increase of the microwave electric field output to 42 W increased the temperature of the activated carbon to 1000 °C. In contrast, under  $H$ -field heating conditions with 17 W microwaves, the temperature rose to 200 °C, 323 °C at 30 W output power, 381 °C at 40 W, and 444 °C at 50 W. When the microwaves'  $H$ -field output was increased to 145 W, the activated carbon temperature increased to 855 °C. Although the heating efficiency of activated carbon by  $H$ -field heating is lower than that of  $E$ -field heating, it is clear that the AC particulates could be heated sufficiently even under magnetic field heating conditions.

Next, the activated carbon temperature was heated to 700 °C by  $E$ -field irradiation in the presence of flowing water (0.1



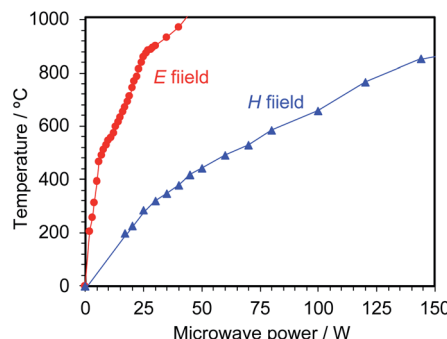


Fig. 3 Temperature change of the AC particulates in the 4 mm quartz reactor with respect to the microwave output power under *E*-field and *H*-field microwave heating conditions in the single-mode applicator.

$\text{mL min}^{-1}$ ) introduced to monitor the formation of hydrogen gas. After about 3 min of microwave irradiation, the reflected power of the microwave increased significantly with some fluctuations likely due to changes in the microwave resonance. The changes were due to the formation of a significant gap in the center of the layer containing the activated carbon, with the upper AC particulates slipping down (see Fig. 4a). This gap formed as a result of the activated carbon being consumed by the steam reforming of water. To the extent that the gap in the activated carbon layer consists of water vapor only, we consider that it caused the dielectric constant and dielectric loss of the entire reactor to partially change, and consequently affected the resonance matching of the microwaves. In another experiment without running water, the temperature distribution of the activated carbon layer ( $<45 \mu\text{m}$ ; 0.12 g; sealed in the quartz vessel) was monitored by thermography immediately after taking out the vessel from the single-mode applicator (Fig. 4b) subsequent to microwave electric field heating up to  $720^\circ\text{C}$ . Note that in this experiment, the amount of activated carbon was decreased by half (0.06 g) to reduce the temperature distribution of the activated carbon layer. Nonetheless, despite reducing the amount of activated carbon by half, we observed

the center of the activated carbon layer to be the hottest as a result of the microwave heating. This strongly infers that the place where the reaction of the activated carbon layer takes place is at the center, with steam reforming proceeding mostly at this location. We further infer that the heat of the heated activated carbon is trapped at the center being unable to escape to its surroundings, unlike the heat of the activated carbon at the two extremes in line with our observations in an earlier study.<sup>12</sup>

Whenever a large temperature inequality occurs in the activated carbon layer, the absorption rate of microwaves with respect to the sample changes significantly causing instability in the microwave resonance. As a result, hydrogen generation is also unstable. A way to resolve this issue is to increase the amount of activated carbon by increasing the size of the reactor, and even if heat distribution due to microwave heating occurred, disperse it so as to diffuse the local thermal energy. Accordingly, an experiment was conducted next under electric field heating using a 16 mm quartz tube reactor (Fig. 1d(ii)).

### 3.3 Hydrogen formation using the 16 mm reactor

The activated carbon particulates (4.5 g) were placed in the 16 mm reactor vessel followed by addition of running ion-exchanged water at a flow rate of  $0.1 \text{ mL min}^{-1}$ . The relationship between microwave input power and the temperature of the activated carbon is summarized in Fig. 5a. The AC at the maximum microwave *E*-field position was heated to about a temperature of  $465^\circ\text{C}$  with 20 W microwaves and to about  $738^\circ\text{C}$  with 40 W microwaves. In contrast, under *H*-field heating the AC particulates were heated to about  $290^\circ\text{C}$  with 20 W microwaves and to *ca.*  $367^\circ\text{C}$  with 40 W microwaves.

The microwave chemical synthesis apparatus (flexiWAVE, Milestone General KK) equipped with a multi-mode applicator was also used to carry out the process implicating the activated carbon (4.5 g) in the 16 mm reactor together with running ion-exchanged water introduced at a rate of  $0.1 \text{ mL min}^{-1}$ . With the multi-mode applicator, the AC particulates could only be heated up to about  $144^\circ\text{C}$  with 100 W microwaves and to *ca.*  $407^\circ\text{C}$  with 400 W microwaves (Fig. 5b); a microwave output power of about 1350 W was required to heat the activated carbon to a temperature of  $700^\circ\text{C}$  with the multi-mode applicator. A simple calculation shows that heating with the microwaves' *E*-field in the single-mode applicator required but 1/36 of the power consumption *vis-à-vis* the multi-mode applicator. Thus, microwave energy is used to obtain hydrogen energy, and to the extent that power consumption for hydrogen generation be kept as low as possible it is evident that the single-mode applicator is the optimal microwave applicator of choice.

### 3.4 Optimized conditions for hydrogen generation (temperature, particle size, flow rate, reactor)

To verify the optimal conditions for hydrogen generation, we began by adding the activated carbon AC in a sealed 16 mm quartz reactor located at the maximal position of the electric field in the single-mode applicator, following which microwave electric field heating was performed while introducing ion-

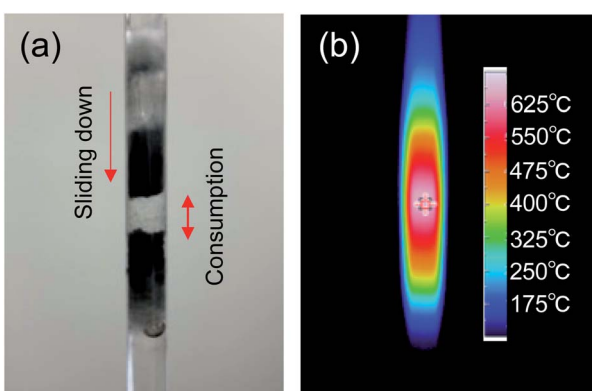


Fig. 4 (a) Photograph of the AC ( $<45 \mu\text{m}$ , 0.12 g) layer in the quartz reactor in the presence of running water ( $0.1 \text{ mL min}^{-1}$ ) after microwave irradiation; (b) image of the temperature distribution monitored by thermography (no running water).



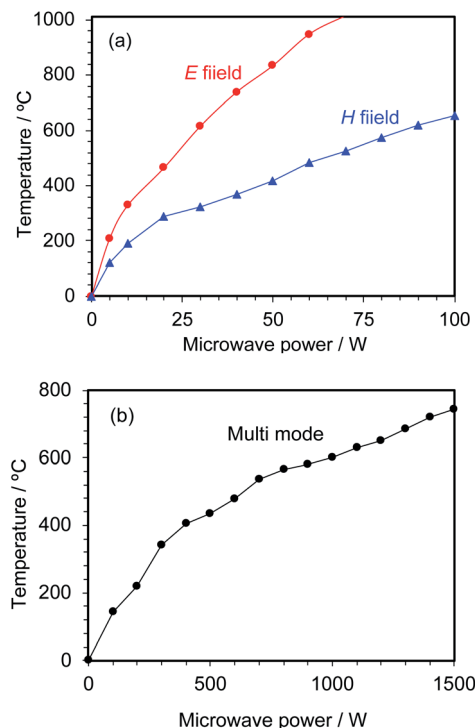


Fig. 5 Temperature change of the AC particulates in the 16 mm quartz reactor with respect to microwave output power under (a) *E*-field and *H*-field microwave heating conditions in the single-mode applicator; (b) temperature distribution in the multi-mode applicator (flexiWAVE Milestone General KK).

exchanged water at a flow rate of  $0.1 \text{ mL min}^{-1}$ . The amount of hydrogen generated was investigated under various temperature conditions. The temperature at the center of the activated carbon layer in the reactor was changed from  $600 \text{ }^\circ\text{C}$  to  $800 \text{ }^\circ\text{C}$ , and the reaction temperature and the amount of hydrogen generated were then compared as illustrated in Fig. 6a. More than 70% of hydrogen was generated after 8 min of microwave irradiation at a temperature of  $600 \text{ }^\circ\text{C}$ . In general, it is well known that almost no hydrogen is generated in chemical equilibrium unless a catalyst is used for steam reforming at a reaction temperature of about  $600 \text{ }^\circ\text{C}$ ,<sup>17</sup> while using the method described herein more than 70% of hydrogen is generated continuously when the activated carbon temperature is  $600 \text{ }^\circ\text{C}$ . This contrast is due to the selective heating of AC by the microwaves as the activated carbon is directly heated without depending on heat conduction. For instance, in our previous study,<sup>12</sup> the Pt/AC catalyst in methylcyclohexane was selectively heated by the microwaves with the temperature difference between the bulk temperature (measured using a thermometer) and the Pt/AC catalyst was estimated as  $217 \text{ }^\circ\text{C}$  from a simulation analysis of electric heating. In other words, the microwaves heated the activated carbon directly, with the heat escaping to the surrounding atmosphere, so that the temperature of the activated carbon was far greater than the bulk temperature. In general, however, in conventional heating, heating proceeds by heat conduction so that the temperature of the activated carbon and the temperature of the bulk tend to be

slightly lower for the activated carbon, while the temperature distribution is opposite. Accordingly, the reason why the steam reforming reaction proceeded sufficiently at  $600 \text{ }^\circ\text{C}$  by this method is that the microscopic temperature of the surface of the activated carbon, which is the reaction field, is greater than the temperature of the bulk system (measured by a thermometer).

Next, we considered the optimal reaction temperature of the method described herein. The hydrogen generation rate fluctuated when the AC was heated at  $600 \text{ }^\circ\text{C}$ . On the other hand, the hydrogen generation rate was stable and improved at  $650 \text{ }^\circ\text{C}$ , although the generation rate temporarily decreased after 18 min of microwave irradiation as observed even after repeating the experiment several times. Accordingly, we set the temperature of activated carbon at  $700 \text{ }^\circ\text{C}$ , which led to a stable generation of hydrogen as also occurred at the higher temperatures (see Fig. 6a).

The optimal conditions with regard to the particle size of the activated carbon for hydrogen generation were examined and are shown in Fig. 6b in terms of % yields. Activated carbon particles with sizes less than  $45 \mu\text{m}$  to  $1.7 \text{ mm}$  were enclosed in the  $16 \text{ mm}$  reactor, and ion-exchanged water was introduced at a flow rate of  $0.1 \text{ mL min}^{-1}$ . The packed AC was heated under microwave *E*-field conditions. In each case the AC introduced matched by the volume to a height of  $50 \text{ mm}$  in the reactor. The reaction temperatures at the center of the activated carbon layers in the reactor were fixed at  $700 \text{ }^\circ\text{C}$ . Results showed that the hydrogen generation yields were similar when the activated carbon particle size was between  $45 \mu\text{m}$  and  $710 \mu\text{m}$ . On the other hand, with activated carbon of particulates greater than  $710 \mu\text{m}$ , the yields of hydrogen were lower up to 10 min of microwave irradiation. As well, hydrogen generation after 10 min of microwave irradiation was not stable with the  $1.7 \text{ mm}$  activated carbon particulates. Monitoring the microwave reflection at this time showed that the reflected output was not constant; microwave resonance had changed. Destabilization of the resonance was caused by the particle size of the activated carbon that when large, the water vapor tends to accumulate in the space between the particles. This resulted in the formation of a gap that led the activated carbon to collapse, thereby leading to a remarkable change in the dielectric factor in the reactor.

We next examined the effect of flow rate of the running water through the reactor on the yields of hydrogen generated. For this experiment, the activated carbon AC ( $<45 \mu\text{m}$ ) was sealed in the  $16 \text{ mm}$  quartz reactor fixed at the maximal position of the *E*-field in the single-mode applicator. Three flow rates of ion-exchanged water flow were examined:  $0.1 \text{ mL min}^{-1}$ ,  $0.3 \text{ mL min}^{-1}$  and  $0.6 \text{ mL min}^{-1}$ . The yields of hydrogen generated under electric field heating conditions with flow rate revealed that from 10 to 40 min of microwave irradiation the average yields were about 75% at a flow rate of  $0.1 \text{ mL min}^{-1}$ , 69% for  $0.3 \text{ mL min}^{-1}$  and 64% for  $0.6 \text{ mL min}^{-1}$  (Fig. 6c). Clearly, increasing the flow rate of water decreased the conversion rate of water into hydrogen gas. On the other hand, reducing the flow rate reduces the efficiency of water decomposition, but increases the amount of hydrogen obtained. The hydrogen gas



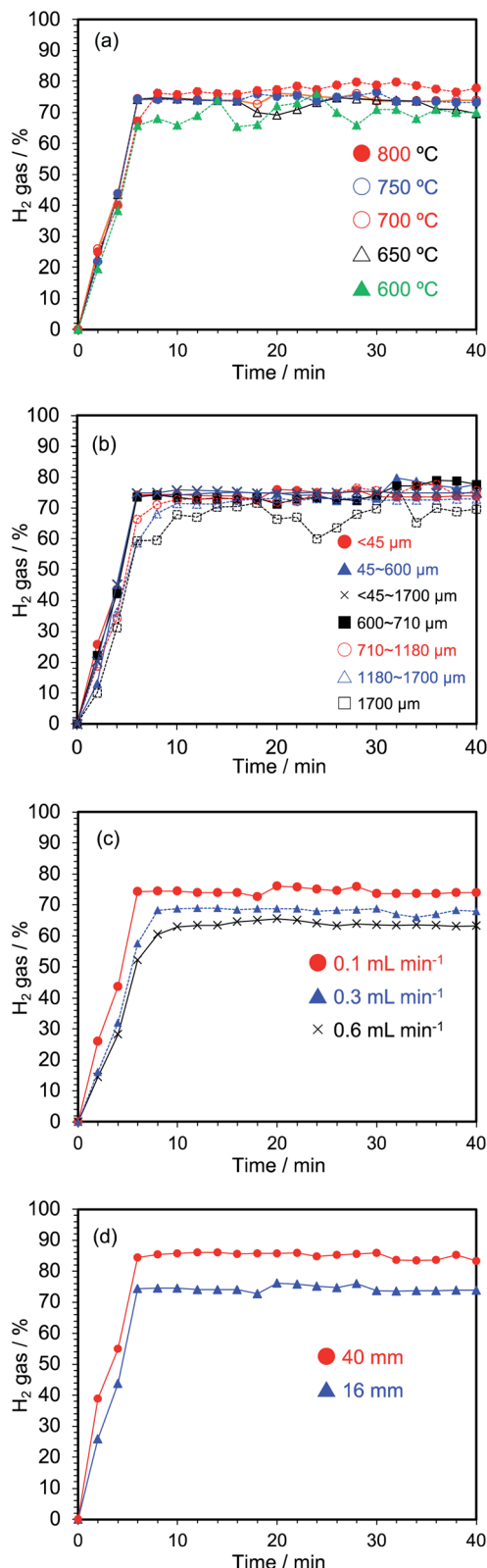


Fig. 6 (a) Examination of optimum conditions for hydrogen generation yields using steam reforming and water–gas shift reaction with activated carbon and water; (b) examination of minimum conditions for the particle size of activated carbon used; (c) optimal flow rate of water; (d) comparison of hydrogen gas generation yields with respect to size of reactor.

produced at a water flow rate of  $0.1 \text{ mL min}^{-1}$  is theoretically generated at  $0.009 \text{ mL min}^{-1}$  (volume of hydrogen gas per min). The flow rate of  $0.3 \text{ mL min}^{-1}$  theoretically generated  $0.026 \text{ mL min}^{-1}$  of hydrogen, while the flow rate of  $0.6 \text{ mL min}^{-1}$  theoretically yielded at  $0.049 \text{ mL min}^{-1}$  of hydrogen. In addition, to the extent that undecomposed water is discharged from the reactor in the form of water, it can be decomposed repeatedly by a multi-cycle process.

The optimal size of the reactor for hydrogen generation was examined using both the 16 mm and the 40 mm reactor vessels in both cases using  $<45 \mu\text{m}$  particulates of the activated carbon and running water at a flow rate of  $0.1 \text{ mL min}^{-1}$  exposed to microwave electric field heating; the mass of the activated carbon was 11.2 g in the 40 mm reactor and 4.5 g in the 16 mm reactor (2.5 times less in the latter). After 2 min of microwave irradiation, the hydrogen gas generation rate in the 16 mm reactor was about 25%, whereas it was *ca.* 39% in the 40 mm reactor (Fig. 6d). However, after 10 min the average hydrogen generation rate in the 40 mm reactor was 86%.

To briefly summarize then, the results displayed in Fig. 6 indicate that it is optimal to use activated carbon particulates with sizes less than  $710 \mu\text{m}$  at a temperature of  $600 \text{ }^\circ\text{C}$  or higher to generate hydrogen using the water reforming reaction driven by the microwaves. As well, if the efficiency of water decomposition were the objective of the experiment, then a flow rate of  $0.1 \text{ mL min}^{-1}$  would be desirable; however, if the volume of hydrogen generated were the goal of the experiment, then a water flow rate of  $0.6 \text{ mL min}^{-1}$  would be necessary. In addition, the efficiency of hydrogen generation was best when the process was carried out in the 40 mm reactor (Fig. 6(d)).

### 3.5 Comparison of the microwave *versus* conventional heating

**3.5.1 *E*-Field and *H*-field heating *versus* conventional heating.** To demonstrate the advantages of microwave heating in generating hydrogen from water, experiments were performed to compare that method with the more traditional method of carrying out steam reforming and/or the water–gas shift processes. Thus, activated carbon particulates (4.5 g) were sealed in the 16 mm quartz reactor that was fixed at the maximal positions of the *E*-field or *H*-field of the single-mode applicator, following which the ion-exchanged water was introduced at a flow rate of  $0.1 \text{ mL min}^{-1}$ . For comparison, hydrogen generation *via* the conventional heating method was also carried out in an electric furnace. In both cases, the reaction temperature was set to  $700 \text{ }^\circ\text{C}$ . Experiments using microwave *H*-field heating showed that the hydrogen generation efficiency was somewhat greater to *E*-field heating by up to 6%. However, as seen from Fig. 5a, there is a large difference in microwave power consumption for heating at  $700 \text{ }^\circ\text{C}$  under *H*-field conditions so that magnetic field heating is not an effective method in terms of electrical energy consumed.

On the other hand, under conventional heating (CH) in a preheated ( $700 \text{ }^\circ\text{C}$ ) ceramic heater-type electric furnace, no hydrogen generation occurred until after a 10 min delay to allow the AC particulates to reach that temperature, after which

hydrogen generation was fairly rapid (Fig. 7a). After 14 min of heating in the electric furnace, the yield of hydrogen generated was similar to those of the microwave method. This result would infer that the rate-determining factor of the process is thermal. In terms of energy expended to produce hydrogen, the power consumption in the electric furnace was 63 W *versus* a power consumption of 37 W (on average) with microwave electric field heating, a 59% reduction in electrical energy in the latter method.

**3.5.2 Effect of added platinum catalyst on activated carbon.** Subsequent to the above, it was relevant to examine the effect of an added catalyst such as Pt supported on activated carbon (5 wt% Pt; Pt particle size: 1–5 nm; Pt/AC size <45  $\mu\text{m}$ ) with regard to yields of hydrogen generated. The initial generation of hydrogen gas using Pt/AC tended to be slower than for pristine activated carbon (see Fig. 7b). It is not unlikely that the hydrogen generated from water in the initial stage was adsorbed onto the Pt particles on the Pt/AC catalyst, which caused a delay in the detection of hydrogen evolved. In addition, with magnetic field heating, more hydrogen was generated (yield = 86%) after 14 min of microwave irradiation. However, hydrogen evolution was significantly reduced on continued magnetic field heating, which we are tempted to attribute to a recombination of hydrogen with oxygen occurring on the platinum surface. But

why this occurs only under microwave *H*-field heating remains elusive at this time. Nonetheless, for the purpose of this study, the use of the Pt/AC catalyst presents no advantages with respect to the use of pristine activated carbon in terms of high hydrogen production yields, cost of platinum and stability of hydrogen evolution.

Clearly then, hydrogen can be generated efficiently from water even under magnetic field heating, but it is inferior to electric field heating from the viewpoint of power consumption. The microwave method can reduce significantly the power consumption as compared to the conventional method. Moreover, the addition of a noble metal catalyst such as Pt supported on AC provides no advantages over pristine activated carbon.

Nonetheless, as the water-gas shift reaction (eqn (4)) is a reversible process, the inverse gas-shift reaction was also examined using a nickel catalyst supported on activated carbon (Ni/AC). The preparation of Ni/AC particles (<45  $\mu\text{m}$ ) involved washing the AC with water and then drying at 70 °C first, followed by refluxing the AC particles in a  $\text{HNO}_3$  aqueous solution (5.0 M) at 80 °C for 6 h. Subsequent to their filtration, the ACs were then immersed in a  $\text{Ni}(\text{NO}_3)_2$  aqueous solution (1.0 M) and stirred for 24 h and dried. The use of Ni/AC as the catalyst revealed a clear decrease in the hydrogen generation yields (*ca.* 45–50%) relative to the yields of hydrogen produced from pristine AC alone (*ca.* 75%) – see Fig. 7b. Apparently, Ni promotes the reverse water-gas shift reaction (eqn (6)) and inhibits the dehydrogenation of water. Consequently, the production of hydrogen *via* steam reforming and water-gas shift reactions by the microwave-driven decomposition of water with AC particulates alone appears far more promising.

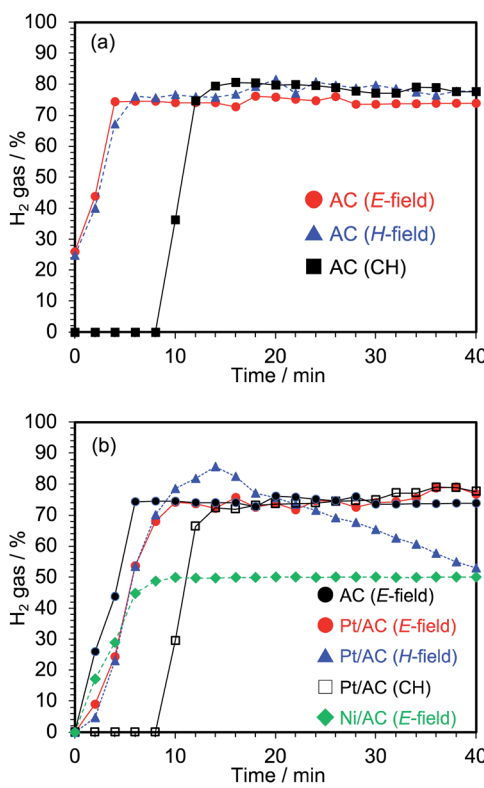


Fig. 7 (a) Hydrogen gas generation yields in the 16 mm quartz reactor with activated carbon (<45  $\mu\text{m}$ ); (b) 5 wt% platinum (1–5 nm) supported on activated carbon (Pt/AC; <45  $\mu\text{m}$ ) and 1 wt% nickel (3–15 nm) supported on activated carbon (Ni/AC; <45  $\mu\text{m}$ ) subjected to microwave *E*-field and *H*-field irradiation – conventional heating was also carried out in a ceramic electric tube furnace for comparison.

### 3.6 Environmentally-based hydrogen generation using spent activated carbon, contaminated water, and seawater

We next conducted experiments using spent activated carbon (coconut shell activated carbon) from an industrial waste to generate hydrogen by the microwave heating method, and in which the AC had been used in water purification and sewage treatments. An EDX elemental analysis of this spent activated carbon revealed that the particulates consisted of 99.68% C, 0.20% S, 0.010% Zn, 0.072% K, 0.027% Cu, and 0.011% Fe. The particle size distribution of this waste activated carbon was also examined using a sieve; the spent activated carbon consisted of 0.019 wt% of particles with size <45  $\mu\text{m}$ , 1.52 wt% of 45–600  $\mu\text{m}$ , 4.71 wt% of 600–710  $\mu\text{m}$ , 55.73 wt% of 0.71–1.18 mm, 36.94 wt% of 1.18–1.7 mm, and 1.08 wt% of 1.7 mm or greater. The spent activated carbon was thus sealed in the 16 mm reactor followed by microwave electric field heating and running ion-exchanged water at a flow rate of 0.10 mL min<sup>-1</sup> with continuous detection of hydrogen evolved by gas chromatography – results from the use of spent AC/H<sub>2</sub>O and pristine AC/H<sub>2</sub>O are reported in Fig. 8a. The initial rate of hydrogen evolution was faster with the spent activated carbon; after about 5 min the yield was essentially the same as for the pristine

coconut shell activated carbon. The center of the particle size distribution of the spent activated carbon was 0.71–1.7 mm, which according to the results presented in Fig. 6b this particle size of more than 0.710 mm was disadvantageous for hydrogen generation. Presumably, because the spent activated carbon contains various particle sizes, we considered it unlikely that a gap was produced within the activated carbon layer as AC particles smaller than 0.71 mm would rapidly fill the void thereby avoiding destabilization and reduction of hydrogen generation.

The possibility of generating hydrogen from an aqueous model wastewater was investigated using an aqueous solution of the water-soluble polyvinyl alcohol (PVA), and an aqueous solution of the insecticide 2,4-dichlorophenoxy acetic acid (2,4-D). Thus, 4.5 g of activated carbon was sealed in the 16 mm reactor followed by microwave electric field heating while introducing the aqueous solutions at the flow rate of 0.1  $\text{mL min}^{-1}$ ; results of the yields of hydrogen evolved are displayed in Fig. 8b. Unexpectedly, hydrogen was generated more rapidly from contaminated waters and artificial seawater than from ion-exchanged water. No doubt, hydrogen was likely also generated from these organic substances, so that even wastewaters present some advantages over ion-exchanged water. In

the case of PVA-contaminated wastewater, conversion of the wastewater was 81% after 6 min of microwave *E*-field heating.

Furthermore, an experiment on hydrogen generation using simulated seawater was also conducted. Recall that electrolysis of water is the most used method to produce hydrogen from water. However, electrolyzing seawater presents some problems as the electrodes used in the electrolysis are corroded by the salt. Inasmuch as the microwave method avoids the use of electrodes, it seems advantageous to use it. Nonetheless, the problem of corrosion of electrodes in the electrolysis of seawater to produce hydrogen and oxygen was resolved by Kuang *et al.*<sup>18</sup> who used a highly corrosion resistant hierarchical anode consisting of a nickel–iron hydroxide electrocatalyst layer uniformly coated on a sulfide layer formed on the Ni substrate. In the present study, the artificial seawater used in tropical fish tanks was used with the main components being sodium chloride, magnesium chloride, potassium chloride, calcium chloride, magnesium sulfate, sodium sulfate, and a chlorine neutralizer.

To the extent that the artificial seawater contains many ions, microwave heating is nonetheless likely to proceed. The component that governs the heating by the microwave *E*-field is the dielectric loss ( $\epsilon''$ ), which consists of two terms: dielectric heating (first term in eqn (7)) and Joule heating (second term in eqn (7)).<sup>19</sup>

$$\epsilon'' = \frac{\epsilon_s - \epsilon_\infty}{1 + \omega^2 \tau^2} \omega \tau + \frac{\sigma}{\omega} \quad (7)$$

where  $\epsilon_s$  is the dielectric constant at low frequencies and  $\epsilon_\infty$  is the dielectric constant at high frequencies,  $\omega$  is the angular frequency of the electromagnetic radiation,  $\sigma$  is the ionic conductivity of the electrolyte solution, and  $\tau$  is the relaxation time taken as a measure of the time required for water to rotate; that is  $\tau = 4\pi\eta r^3/\kappa T$ , where  $r$  is the molecular radius,  $\kappa$  is Boltzmann's constant,  $T$  is the Kelvin temperature, and  $\eta$  is the viscosity that may be considered to cause the delay of molecules (or particles) to respond to the field changes.

The second term in eqn (7) is responsible for the temperature rise of water because seawater was sufficiently heated by Joule heating. Therefore, the initial hydrogen generation was very fast, and was greater than that of pure water (Fig. 8b). When the activated carbon was analyzed after the reaction by energy dispersive X-ray spectroscopy (EDX), elements such as Mg, Na, Cl, Ca, and S were observed; the corresponding ions in the artificial seawater were likely trapped in the activated carbon.

## 4. Concluding remarks

This article has described the serendipitous discovery that hydrogen can be extracted from ambient water without using electrodes *via* the selective heating of the activated carbon catalyst by microwaves at 600 °C (optimal temperature, 700 °C), a temperature generally considered low to carry out steam reforming and water–gas shift processes that we inferred to be the processes involved in extracting hydrogen from ion-exchanged water, wastewaters and seawater under microwave irradiation – the novel method *vis-à-vis* the more conventional

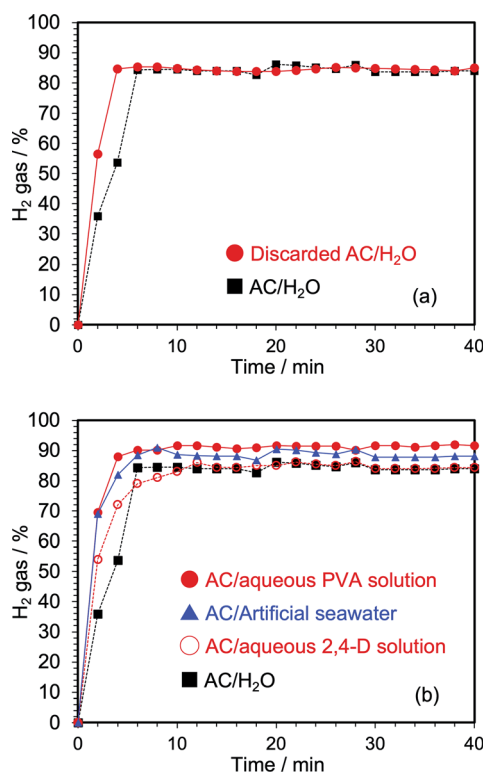


Fig. 8 Hydrogen gas generation yields with a 16 mm quartz reactor with (a) activated carbon (<45  $\mu\text{m}$ ) and activated waste carbon of various sizes with ion-exchange water and (b) using an aqueous polyvinyl alcohol (PVA) solution, as well with an aqueous 2,4-dichlorophenoxy acetic acid (2,4-D) solution, artificial seawater and ion-exchanged water; the size of the activated carbon was <45  $\mu\text{m}$  exposed to microwave *E*-field heating.

heating method. The use of microwaves causes a 59% lower power consumption rate with respect to conventional heating. Evidently, the activated carbon extracts oxygen from water to generate hydrogen and carbon dioxide. As well, to the extent that the generation of hydrogen gas and the generation of carbon dioxide proceed at the same time, there is a trade-off relationship between energy acquisition and global warming. However, we hasten to point out that the use of spent activated carbon leads to the re-use of activated carbon, thus eliminating the disposal of this material that had been used in water and sewage treatments. Moreover, as the activated carbon is produced from plant biomass raw materials, the carbon dioxide produced falls under the notion of carbon neutrality wherein plants absorb and circulate carbon.<sup>20</sup> Accordingly, the amount of carbon dioxide in the atmosphere neither increases nor decreases. As an example, the amount of spent activated carbon in Japan is 47 000 tons per year, which is typically incinerated or otherwise disposed of in landfills.<sup>21</sup> If hydrogen energy were extracted from unnecessary activated carbon in combination with wastewaters, then the novel method described herein can contribute to some resolution of the energy problem. Moreover, if microwaves were generated with a renewable energy source, such as sunlight, then the microwave method could be connected to small- to medium-sized hydrogen stations.

## Authors' contributions

S. H. planned the research, summarized the data, and wrote the first draft; R. T., K. S., and H. T. performed the experiments; S. H. and N. S. examined, interpreted the data, and wrote final draft.

## Conflicts of interest

Authors have no conflicts of interest to declare.

## Acknowledgements

We are grateful to the Japan Society for the Promotion of Science (JSPS) for financial support through a Grant-in-aid for Scientific Research to S. H. (No. 19K22316). One of us (NS) thanks the staff of the PhotoGreen Laboratory of the University of Pavia, Italy, for their continued hospitality.

## Notes and references

- 1 A. Zuüttel, Hydrogen storage methods, *Naturwissenschaften*, 2004, **91**, 157–172.
- 2 E. Katz, Electrochemical contributions: William Nicholson (1753–1815), *Electrochem. Sci. Adv.*, 2021, **1**, e2160003.
- 3 J. Gretz, J. P. Baselt, O. Ullmann and H. Wendt, The 100-MW Euro-Quebec hydro-hydrogen pilot project, *Int. J. Hydrogen Energy*, 1990, **15**, 419–424.
- 4 A. Fujishima and K. Honda, Electrochemical Photolysis of Water at a Semiconductor Electrode, *Nature*, 1972, **238**, 37–38.

- 5 K. Onuki, H. Noguchi, N. Tanaka, H. Takegami and S. Kubo, Thermochemical decomposition of water, *Surf. Sci.*, 2015, **36**, 80–85.
- 6 N. Serpone, A. V. Emeline, V. K. Ryabchuk, V. N. Kuznetsov, Y. M. Artem'ev and S. Horikoshi, Why do Hydrogen and Oxygen Yields from Semiconductor-Based Photocatalyzed Water Splitting Remain Disappointingly Low? Intrinsic and Extrinsic Factors Impacting Surface Redox Reactions, *ACS Energy Lett.*, 2016, **1**, 931–948.
- 7 (a) F. E. Osterloh and B. A. Parkinson, Recent developments in solar water-splitting photocatalysis, *MRS Bull.*, 2011, **36**, 17–22; (b) C.-H. Liao, C.-W. Huang and J. C. S. Wu, Hydrogen Production from Semiconductor-based Photocatalysis via Water Splitting, *Catalysts*, 2012, **2**, 490–516; (c) K. Kalyanasundaram, Photochemical applications of solar energy: Photocatalysis and photodecomposition of water, *Photochemistry*, 2013, **41**, 182–265; (d) S. Prott, A. Albini and N. Serpone, Photocatalytic generation of solar fuels from the reduction of  $H_2O$  and  $CO_2$ : a look at the patent literature, *Phys. Chem. Chem. Phys.*, 2014, **16**, 19790; (e) V. K. Ryabchuk, V. N. Kuznetsov, A. V. Emeline, Y. M. Artem'ev, G. V. Kataeva, S. Horikoshi and N. Serpone, Water Will Be the Coal of the Future—The Untamed Dream of Jules Verne for a Solar Fuel, *Molecules*, 2016, **21**, 1638; (f) B. Gupta and A. A. Melzin,  $TiO_2$ /RGO composites: Its achievement and factors involved in hydrogen production, *Renewable Sustainable Energy Rev.*, 2017, **76**, 1384–1392; (g) Y. Wu and L. Bi, Research Progress on Catalytic Water Splitting Based on Polyoxometalate/Semiconductor Composites, *Catalysts*, 2021, **11**, 524.
- 8 S. Horikoshi and N. Serpone, Role of microwaves in heterogeneous catalytic systems, *Catal. Sci. Technol.*, 2014, **4**, 1197–1210.
- 9 X. Jie, W. Li, D. Slocombe, Y. Gao, I. Banerjee, S. Gonzalez-Cortes, B. Yao, H. A. Megren, S. Alshihri, J. Dilworth, J. Thomas, T. Xiao and P. Edwards, Microwave-initiated catalytic deconstruction of plastic waste into hydrogen and high-value carbons, *Nat. Catal.*, 2020, **3**, 902–912.
- 10 S. Czernik, R. French, C. Feik and E. Chornet, Production Of Hydrogen From Post-Consumer Wastes, *Proceedings of the 2002 U.S. DOE Hydrogen Program Review NREL/CP-610-32405*, National Bioenergy Center, National Renewable Energy Laboratory, Golden, Colorado, USA 80401, <https://www.nrel.gov/docs/fy02osti/32405a9.pdf>, accessed July 23, 2021.
- 11 L. Collins, *Turning plastic waste into hydrogen: first commercial plant moves step closer*, January 7, 2020, see <https://www.rechargenews.com/transition/turning-plastic-waste-into-hydrogen-first-commercial-plant-moves-step-closer/2-1-733678>, accessed July 23, 2021.
- 12 S. Horikoshi, M. Kamata, T. Sumi and N. Serpone, Selective heating of Pd/AC catalyst in heterogeneous systems for the microwave-assisted continuous hydrogen evolution from organic hydrides: Temperature distribution in the fixed-bed reactor, *Int. J. Hydrogen Energy*, 2016, **41**, 12029–12037.
- 13 S. Horikoshi, T. Watanabe, A. Narita, Y. Suzuki and N. Serpone, The electromagnetic wave energy effect(s) in



microwave-assisted organic syntheses (MAOS), *Sci. Rep.*, 2018, **8**, 5151, DOI: 10.1038/s41598-018-23465-5.

14 N. J. Cronin, *Microwave and Optical Waveguides*, Institute of Physics Publishing, Bristol, UK, 1995, pp. 27–40.

15 S. Horikoshi, A. Matsubara, S. Takayama, M. Sato, F. Sakai, M. Kajitani, M. Abe and N. Serpone, Characterization of microwave effects on metal-oxide materials: Zinc oxide and titanium dioxide, *Appl. Catal., B*, 2009, **91**, 362–367.

16 S. Horikoshi, T. Sumi and N. Serpone, Unusual effect of the magnetic field component of the microwave radiation on aqueous electrolyte solutions, *J. Microwave Power*, 2012, **46**, 215–228.

17 S. Egashira, Low temperature steam reforming process of petroleum hydrocarbons, *J. Fuel Soc. Jpn.*, 1967, **46**, 508–513.

18 Y. Kuang, M. J. Kenney, Y. Meng, W.-H. Hung, Y. Liu, J. E. Huang, R. Prasanna, P. Li, Y. Li, L. Wang, M.-C. Lin, M. D. McGehee, X. Sun and H. Dai, Solar-driven, highly sustained splitting of seawater into hydrogen and oxygen fuels, *Proc. Natl. Acad. Sci.*, 2019, **116**, 6624–6629.

19 S. Horikoshi, R. F. Schiffmann, J. Fukushima and N. Serpone, *Microwave chemical and materials processing. A tutorial*, Springer Nature, Singapore Pte Ltd., 2018, DOI: 10.1007/978-981-10-6466-1.

20 See for example, [https://en.wikipedia.org/wiki/Carbon\\_neutrality](https://en.wikipedia.org/wiki/Carbon_neutrality), accessed July 23, 2021.

21 From materials provided by the Organo Corporation, Koto-ku, Tokyo, Japan.

